Computer Modeling in Engineering & Sciences CMES, vol.123, no.3, pp.1205-1222, 2020

Modeling Tracer Flow Characteristics in Different Types of Pores: Visualization and Mathematical Modeling

Tongjing Liu[1, 2, *], Weixia Liu[3], Pengxiang Diwu[4], Gaixing Hu[5, 6], Ting Xu[1, 7], Yuqi Li[2], Zhenjiang You[8], Runwei Qiao[2] and Jia Wang[2]

Abstract: Structure of porous media and fluid distribution in rocks can significantly affect the transport characteristics during the process of microscale tracer flow. To clarify the effect of micro heterogeneity on aqueous tracer transport, this paper demonstrates microscopic experiments at pore level and proposes an improved mathematical model for tracer transport. The visualization results show a faster tracer movement into movable water than it into bound water, and quicker occupancy in flowing pores than in storage pores caused by the difference of tracer velocity. Moreover, the proposed mathematical model includes the effects of bound water and flowing porosity by applying interstitial flow velocity expression. The new model also distinguishes flowing and storage pores, accounting for different tracer transport mechanisms (dispersion, diffusion and adsorption) in different types of pores. The resulting analytical solution better matches with tracer production data than the standard model. The residual sum of squares (RSS) from the new model is 0.0005, which is 100 times smaller than the RSS from the standard model. The sensitivity analysis indicates that the dispersion coefficient and flowing porosity shows a negative correlation with the tracer breakthrough time and the increasing slope, whereas the superficial velocity and bound water saturation show a positive correlation.

Keywords: Tracer flow characteristics, different types of pores, interstitial flow velocity, visualization and mathematical modeling, tracer concentration prediction model.

[1] State Energy Center for Shale Oil Research and Development, Beijing, 100083, China.
[2] Unconventional Petroleum Research Institute, China University of Petroleum, Beijing, 102249, China.
[3] Research Institute of Petroleum Exploration and Development, Sinopec Shengli Oilfield Company, Dongying, 257015, China.
[4] College of Science, China University of Petroleum, Beijing, 102249, China.
[5] Oil and Gas Technology Institute, PetroChina Changqing Oilfield Company, Xi'an, 710081, China.
[6] National Engineering Laboratory of Low Permeability Oil & Gas Exploration and Development, Xi'an, 710081, China.
[7] Research Institute of Petroleum Exploration and Development, SINOPEC, Beijing, 100083, China.
[8] School of Chemical Engineering, The University of Queensland, Brisbane, QLD 4072, Australia.
* Corresponding Author: Tongjing Liu, Email: ltjcup@cup.edu.cn.

Received: 28 October 2019; Accepted: 17 March 2020.

1 Introduction

Accurate knowledge of reservoir is a key factor for successful reservoir management. The tracer test technology has become an efficient and straightforward tool to determine parameters of interwell channels [Al-Mosa, Zaberi and Huseby (2013); Liu, Jiang, Li et al. (2008); Liu, Zhang, Jiang et al. (2007); Huang, Xu, Fu et al. (2018)]. Tracer concentration curves can offer distinctive insights into the reservoir characteristics and provide an evaluation method for reservoir heterogeneity. Moreover, Liu et al. [Liu, Diwu, Jiang et al. (2013)] and Zha [Zha (2010)] have demonstrated that, adopting necessary optimization algorithm, tracer concentration interpretation can automatically lead to the accurate information of interwell channels including permeability, thickness, and sweep volume. Flow information in water flooding reservoirs [Al-Mosa, Zaberi and Huseby (2013); Liu, Jiang, Li et al. (2007); Zhang, Liu, Zhang et al. (2005); Kam, Han and Datta-Gupta (2016); Al-Shalabi, Luo, Delshad et al. (2015); Huseby, Hartvig, Jevanord et al. (2015)], and gas flooding reservoirs [Jodar, Medina and Carrera (2009); Rein and Schulz (2007); Singh, Pilz, Zimmer et al. (2012); Gilfillan, Sherk, Poreda et al. (2017)] can be obtained by the tracer test technology.

Mennella et al. [Mennella, Bryant and Lockhart (1999); Li, Liu, He et al. (2012); Krogstad, Lie, Nilsen et al. (2017)] applied the Continuous-Time-Random-Walk (CTRW) method, proposed by Scher et al. [Scher and Lax (1973a, 1973b); Stalgorova and Babadagli (2012)], to describe the interactions between tracer and polymer and model tracer transport in polymer flooding reservoirs. Li et al. [Li, Jiang, Li et al. (2011)] showed in the experiment that the surface of rocks and retained polymers can adsorb tracers simultaneously. Yang et al. [Yang and Liu (2007)] ignored adsorption of tracers during tracer modeling, because the used aqueous tracer is close to ideal state and hardly adsorbed by rock surface. For microelement tracers, however, it is unwise to ignore the adsorption effect because of the trivial amount of injected tracers. Yang [Yang (2012)] reported that the adsorbed concentration can significantly affect the produced tracer concentration. Cox et al. [Cox, Alsenani, Miller et al. (2017)] found that besides using novel polymeric nanoparticles to mitigate memory effects and deploy multiple tracers simultaneously in complex oil reservoir, retention or adsorption of it has even greater influence on the produced tracer concentration. Nevertheless, Dindoruk et al. [Dindoruk and Dindoruk (2008); Widiatmojo, Sasaki, Yousefi-Sahzabi et al. (2015)] did not consider the adsorption term in analytical modelling of tracer transport.

Additionally, Semra et al. [Semra, Sardin and Simonnot (2008)] ignored the differences of tracer velocity in different types and sizes of pores, which were considered by Boving et al. [Boving and Grathwohl (2001)] and resulted in discrepancies compared to experimental data for low-porosity cores. Bellin et al. [Bellin and Rinaldo (1995)] found porous media structures and fluid distribution can cause physical and chemical microscale heterogeneity, respectively. Semra et al. [Semra, Sardin and Simonnot (2008)] showed experimentally that microscale heterogeneity is responsible for solute distribution and has a visible effect on breakthroughs. Liu et al. [Liu, Jiang, Liu et al. (2013)] demonstrated that dispersion can

affect tracer distribution on flow and latitudinal direction when cores have strong microscale heterogeneity in the microscopic experiments. Brigham et al. [Brigham, Reed and Dew (1961)] summarized the above features macroscopically into dispersion, which is a function of tracer velocity. It demonstrates the necessity to consider the differences of tracer velocity between different types of pores to obtain accurate results of tracer concentration.

Li et al. [Li, Jiang and Li (2010)] discovered the "Chromatographic effect" in microscopic experiments. It indicates the injected aqueous tracer can be adsorbed by rock surface and enter the bound water, resulting in the tracer flows being slower than movable water. Furthermore, Liu et al. [Liu, Jiang, Liu et al. (2013)] showed this phenomenon becomes conspicuous in highly heterogeneous porous media. It means that water and oil distribution can also affect the tracer distribution during diffusion and dispersion.

The objective of this paper is to improve tracer transport modeling by considering the effects of micro-heterogeneity, i.e., different types of pores and fluid saturation. In Section 2, microscopic experiments are conducted to analyze tracer flow characteristics in flowing and storage pores, especially in movable and bound water. In Section 3, based on the findings in microscopic experiments, the mechanisms of tracer in different types of pores are summarized and characterized mathematically. In Section 4, applying the equations of physical properties, we propose the mathematical model for tracer transport and obtain the analytical solution of tracer concentration, which better matches the tracer concentration curve than old model. In Section 5, sensitivity analysis is conducted to find the trend of tracer concentration with different tracer and fluid properties.

2 Microscopic tracer flow characteristics

2.1 Experimental setup and procedure

In this section, microscopic experiments are conducted to study tracer flow characteristics at pore level. Fig. 1 illustrates the procedure of the microscopic experiments, which is mainly

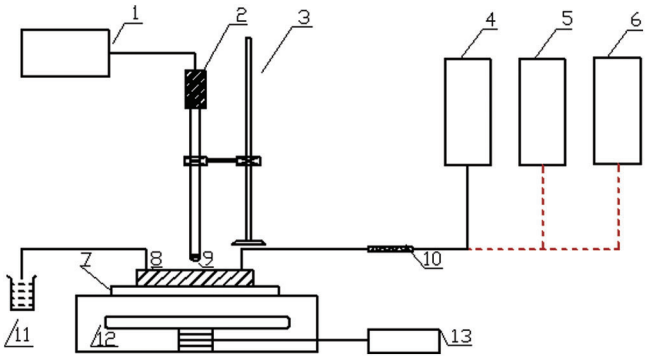

Figure 1: Experimental setup scheme of the tracer transport microscopic experiment 1 Screen, 2 Signal-collecting system, 3 Support unit, 4 Container for tracer, 5 6 Container for water, 7 Glass sheet, 8 Microscopic model, 9 Microscope, 10 Automatic coupling, 11 Container for product liquid, 12 Light source, 13 Power source

constructed by Screen (1), Signal-collecting system (2), Microscopic model (8) and Microscope (9).

The signal-collecting system (2) has imaging speed of 25 frames per second and image resolution of 576×768. The microscopic model (8) is laser etched according an electronic microscope image of real cores. The model is square with length 5 cm, permeability 10-50 D, and pores radius 30-200 μm, which pore volumes (PV) are 0.149 mL measured by weighing method. The microscope (9) has objective multiple as 0.32, 1, and 2, and stepless zoom range from 5 to 40 times.

According to the industry standard SY/T5925-94, methylene-blue solution is recommended to be used in microscopic experiments, which are easy to obtain and convenient for observation in microscopic experiments.

The major experimental procedures are as follows.

(I) Evacuate the microscopic model (8) and then saturate it by water.

(II) Inject 5 PV water as 0.016 mL/min at temperature 25°C.

(III) Inject 5 PV tracer solutions with same rate and temperature in the Step (II). In the displacement Process (II) and (III), Signal-collecting system takes images of the microscopic model with 25 frames per second. Some of the images are shown in Section 2.2.

2.2 Microscopic images

Figs. 2 and 3 illustrate the microscopic model images at different tracer injection volumes. The red and yellow boxes in Figs. 2 and 3 mark the flowing and storage pores, respectively. In the flowing pores, which is connected to more than one adjacent pores, the injected tracer flows along with a very tortuous path and is distributed into movable water as early as 0.04 PV (Fig. 2(a)). This is due to advection of tracer. At 0.89 PV (Fig. 2(b)), the adjacent pores become blue and are occupied by the tracer, while the bound water in relative tight pores is still white. It indicates there are different tracer transport characteristics between the movable and bound water, even in the same flowing pores. The difference between tracer velocities in movable and bound water results in different mechanisms of tracer transport. Lan et al. [Lan (2011); Li (2014)] considered that mechanical dispersion rather than

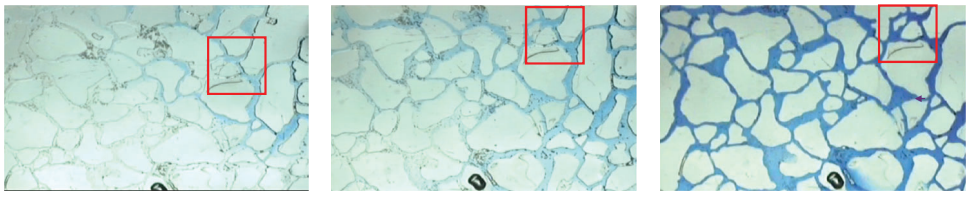

(a) (b) (c)

Figure 2: Images of tracer distribution in the flowing pores of the microscopic model during tracer injection (a) 0.04 PV (b) 0.89 PV (c) 1.43 PV

molecular diffusion controls the tracer distribution at high velocity. At 1.43 PV (Fig. 2(c)), the tracers occupy all pores, which are blue completely.

In the storage pores (yellow box in Fig. 3), which has only one adjacent pore, it is still white after 3.02 PV. Since water cannot flow into the storage pores, there is no advection or dispersion, but only slow diffusion.

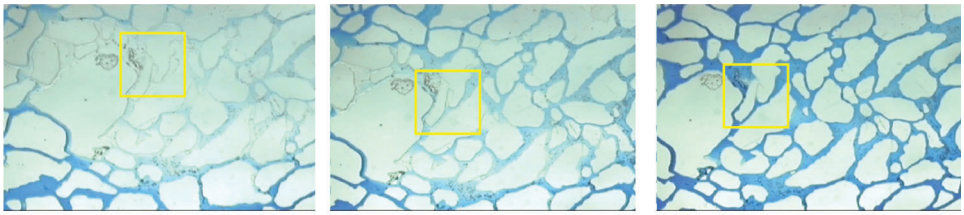

(a) (b) (c)

Figure 3: Images of tracer distribution in the storage pores of the microscopic model during tracer injection: (a) 3.02 PV; (b) 3.83 PV; (c) 5.00 PV

2.3 Results analysis

From Fig. 2, we observe that the injected tracer first occupies movable water and then bound water in the flowing pores. It indicates that there are different forces or mechanisms controlling the tracer concentration distribution in movable and bound water. Based on Fig. 3, the injected tracer cannot occupy the storage pores completely until 5 PV tracer injections. It implies that the mechanism in storage pores are very different from that in flowing pores, because the water flow velocity is zero in storage pores. Therefore, we should consider these characteristics and treat different types of pores separately in tracer transport mathematical modelling.

3 Mechanisms of tracer transport at pore level

Tracers have different transport characteristics not only in movable and bound water, but also in flowing and storage pores. It should be considered in mathematical modelling of tracer transport. Fig. 4 and Tab. 1 illustrate main conceivable action of tracer, which are diffusion and adsorption in storage pores, and advection, dispersion, diffusion and adsorption in flowing pores, respectively. In storage pores, tracer diffuses into the bound water by concentration differences and can be adsorbed onto rock surface. In flowing pores, tracer can adsorb onto rock surface and disperse into movable water by advection, as well as diffuses into bound and movable water.

3.1 Interstitial flow velocity in flowing pores

Interstitial flow velocity in flowing pores can affect the dispersion and play a key role in tracer concentration distribution. The inaccurate real velocity will induce mistakes on evaluation of tracer concentration distribution. As Fig. 3 shows, the aqueous tracer flows

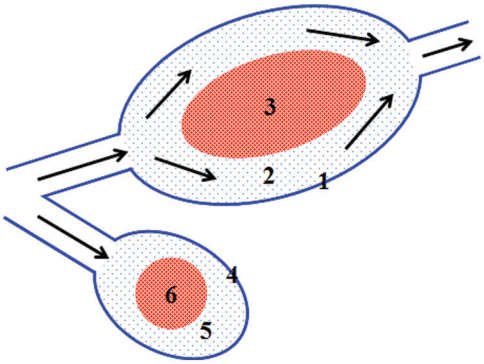

Figure 4: Schematic diagram of a flowing pore and a storage pore 1, 2, 3 are bound water, movable water and oil in flowing pore, respectively; 4, 5 are rock surface, bound water, respectively; 6 is oil in storage pore

Table 1: Main mechanisms of tracer transport in storage and flowing pores

Pore types	Components	Main mechanisms
Storage pores	Bound water	Diffusion
	Rock surface	Adsorption
Flowing pores	Movable water	Advection Dispersion Diffusion
	Bound water	Diffusion
	Rock surface	Adsorption

only in movable water in flowing pores, rather than in the bound water, the oil, and storage pores. Therefore, the tracer interstitial flow velocity in flowing pores should be characterized as follows

$$u = \frac{u'}{\phi_f(1 - S_o - S_{wc})} \tag{1}$$

where u and u' are interstitial and superficial velocities of tracer, respectively, cm/s; u' is the quotient of injection rates and sectional area of cores; Φ_f is flowing porosity, i.e., porosity of flowing pores; S_o and S_{wc} are oil saturation and bound water saturation in flowing pores, respectively.

3.2 Dispersion in flowing pores

Brigham et al. [Brigham, Reed and Dew (1961)] considered that both the dispersion and diffusion can affect the distribution of tracer concentration in flowing pores. The mixing coefficient resulting from dispersion and diffusion is expressed as

$$D = \frac{D_m}{l\phi} + \alpha u^{1.2} \tag{2}$$

where D is mixing coefficient, cm^2/s; D_m is molecular diffusion coefficient, cm^2/s; l is rock tortuosity factor; Φ is total porosity; α is dispersion coefficient, cm.

Li et al. [Li, Jiang and Liu (2010)] found that the dispersion is in line with tracer flow direction while the diffusion is perpendicular to the direction. Li et al. [Li (2014); Huseby, Sagen, Viig et al. (2013)] considered that molecular diffusion is dominant when fluid velocities are close to zero. However, tracers usually transport fast because of high permeability channels or fractures between wells. Therefore, it is reasonable to neglect diffusion and only consider dispersion in flowing pores. Hence, Eq. (2) can be simplified as follows

$$D = \alpha u \tag{3}$$

3.3 Adsorption on rock surface

Hanaor et al. [Hanaor, Ghadiri, Chrzanowski et al. (2014)] showed that tracers can be adsorbed onto rock surface when they flow through porous media. The adsorption could be thought to obey the Langmuir isothermal adsorption law

$$C_r = \frac{aC}{1 + bC} \tag{4}$$

where C_r is adsorbed tracer concentration, mg/g; a, b are the adsorption coefficients; C is tracers concentration in aqueous, mg/L.

Al-Mosa et al. [Al-Mosa, Zaberi and Huseby (2013)] showed that the tracer concentration in porous media is relatively small compared with the huge water swept volume by most tracer tests. Meanwhile, aiming to reduce cost, engineers look forward to injection tracers as little as possible to just meet detection demand. In some field cases, very small tracer amounts are recovered. When the tracer concentration is low, therefore, the adsorption law could be simplified as follows

$$C_r = aC \tag{5}$$

3.4 Diffusion in bound water and storage pores

The tracers are contacted to bound water with a large area and long time, especially in the case of reservoir scale. Therefore, it is assumed that the diffusion makes the distribution in equilibrium ultimately, i.e., concentrations in bound and water phase are equal

$$C_{swc} = C \tag{6}$$

where C_{swc} is tracer concentration in bound water, mg/L.

Considering large sweep pore volume in interwell channels, it is also assumed that concentrations in storage pores and aqueous are equal

$$C_{nonp} = C \tag{7}$$

where C_{nonp} is tracer concentration in storage pores, mg/L.

4 Mathematical models

4.1 Governing equation

Considering one-dimensional flow through the pores shown in Fig. 4, the dispersion occurs in flowing pores only and can be expressed as follows

$$-\frac{\partial u_i}{\partial x}\phi_f(1 - S_o - S_{wc})dxdt \tag{8}$$

where u_{i} is tracer flux velocity caused by dispersion, cm/s; x is distance, cm.

The advection occurs in flowing pores only and can be expressed as follows

$$-u\frac{\partial C}{\partial x}\phi_f(1 - S_o - S_{wc})dxdt \tag{9}$$

The adsorption occurs on rock surface and can be expressed as follows

$$\frac{\partial C_r}{\partial t}(1 - \phi)\rho_r dxdt \tag{10}$$

where ρ_{r} is rock density, g/cm^3.

Assuming the storage pores have the same S_{wc} with flowing pores, then the diffusion term in bound water can be expressed as follows

$$\frac{\partial C_{swc}}{\partial t}\phi S_{wc}dxdt \tag{11}$$

The accumulative mass change in time dt consists of the mass changes in flowing pores and storage pores, respectively

$$\frac{\partial C}{\partial t}\phi_f(1 - S_o - S_{wc})dxdt \tag{12}$$

$$\frac{\partial C_{nonp}}{\partial t}\left(\phi - \phi_f\right)(1 - S_o - S_{wc})dxdt \tag{13}$$

According to the principle of mass conservation, the governing equation of tracer in flowing and storage pores can be expressed as follows

$$\begin{aligned}&-\frac{\partial u_i}{\partial x}\phi_f(1-S_o-S_{wc})-u\frac{\partial C}{\partial x}\phi_f(1-S_o-S_{wc})\\&=\frac{\partial C_{swc}}{\partial t}\phi S_{wc}+\frac{\partial C}{\partial t}\phi_f(1-S_o-S_{wc})+\frac{\partial C_{nonp}}{\partial t}\left(\phi-\phi_f\right)(1-S_o-S_{wc})+\frac{\partial C_r}{\partial t}(1-\phi)\rho_r\end{aligned} \tag{14}$$

Substituting Eqs. (5) to (7) into the governing Eq. (14), yields

$$-\frac{\partial u_i}{\partial x}-u\frac{\partial C}{\partial x}=\frac{[\phi(1-S_o)+a(1-\phi)\rho_r]}{\phi_f(1-S_o-S_{wc})}\frac{\partial C}{\partial t} \tag{15}$$

The tracer mixture velocity can be expressed as

$$\frac{\partial u_i}{\partial x}=\frac{\partial}{\partial x}\left(-D\frac{\partial C}{\partial x}\right) \tag{16}$$

The governing equation of tracer flow at pore level is finally obtained as

$$D\frac{\partial^2 C}{\partial x^2}-u\frac{\partial C}{\partial x}=\frac{[\phi(1-S_o)+a(1-\phi)\rho_r]}{\phi_f(1-S_o-S_{wc})}\frac{\partial C}{\partial t} \tag{17}$$

4.2 Initial and boundary conditions

In the tracer tests, t=0 corresponds to the time of tracer injection. In one-dimensional case, the initial and boundary conditions can be expressed as follows

$$C(x,0)=\begin{cases}C_0 & x\le 0\\ 0 & x>0\end{cases} \tag{18}$$

$$C(0,t)=C_0 \quad t>0 \tag{19}$$

$$C(\infty,t)=0 \quad t>0 \tag{20}$$

where C_o is tracer concentration in injected water, mg/L.

4.3 Analytical solution

Eqs. (17) to (20) complete the mathematical model of tracer flow at pore level. To obtain the analytical solution, the modified time t' is defined as

$$t'=\frac{\phi_f(1-S_o-S_{wc})}{\phi(1-S_o)+a(1-\phi)\rho_r}t \tag{21}$$

By introducing the modified time t′, the mathematical model of tracer flow at pore level is simplified to a typical convective-dispersive solute transport equation consequently [Nihoul and Jacques (1983); Yang, Shao, Zhu et al. (2019)]. Applying the Laplace transform, which

applied by Kocabas [Kocabas (2011)], the analytical solution in real space is obtained as follows

$$\frac{C}{C_0} = \frac{1}{2} erfc\left(\frac{x - ut'}{2\sqrt{Dt'}}\right) + \frac{1}{2} e^{\frac{ux}{2D}} erfc\left(\frac{x + ut'}{2\sqrt{Dt'}}\right) \tag{22}$$

where C/C_o is the tracer concentration ratio.

It is worth noting that replacing t' by t in Eq. (22) leads to the standard model for tracer concentration. The difference between the new model (22) and previous standard model lies in the variable transformation in Eq. (21), which accounting for the effects of flowing porosity and bound water.

4.4 Comparison with standard model

In this section, we conduct a tracer displacement experiment in a sand pack model. Tab. 2 shows the main parameters in the experiment, in which the core porosity is 0.372 while the flowing porosity is 0.23.

Table 2: Basic parameters in the tracer displacement experiment

Core length/cm	25	Core radius/cm	1.25
Tracer injection rate/cm^3s^{-1}	0.02	Rock density/gcm^{-3}	2.4
Oil saturation	0.2	Bound water saturation	0.21
Porosity	0.372	Flowing porosity	0.23

Based on the proposed tracer transport concentration solution (Eq. (22)), that accounting for flowing porosity and bound water effects, the calculated tracer concentration (blue line in Fig. 5) fits the measured tracer concentration very well, and the RSS is 0.0005. When neglecting the effect of flowing porosity and bound water as the standard model does, the calculated tracer concentration (green line in Fig. 5) cannot fit the measured tracer concentration and corresponding RSS is 0.0515, about one hundred times larger of the proposed model.

As Fig. 5 shows, the tracer concentration ratio shows deviation like higher dispersion effect when ignoring effect of flowing porosity and bound water. This phenomenon will result in error of interwell-heterogeneity estimation in tracer field application. To validate the new model in this paper, the new model in this paper is used to the tracer test interpretation with necessary streamline method and optimization algorithm. Fig. 6 illustrates the field matching curves from H shale oil reservoir in China, which reaching application demand. The interpretation results show the average permeability and swept volume of interwell channeling as 105.6 mD and 457 m^3, respectively. These parameters are consistent with the knowledge from the wells production performance.

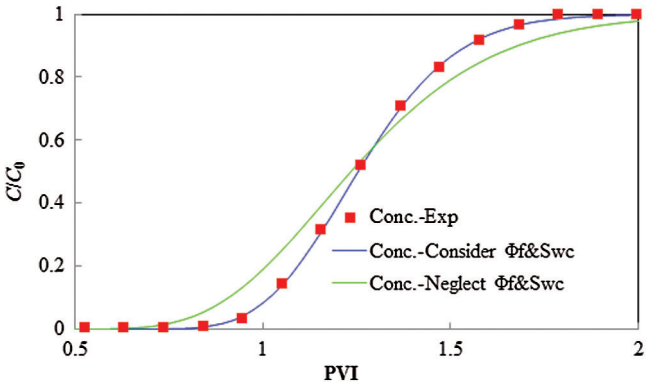

Figure 5: Comparison of experimental and calculated tracer concentration *vs.* injection pore volume (PVI) Conc.-Exp is the tracer concentration tested in the experiments, mg/L; Conc.-Consider Φ_f & S_{wc} is the tracer concentration calculated by the new model; Conc.-Consider Φ_f & S_{wc} is the tracer concentration calculated by the model neglecting flowing porosity and water saturation

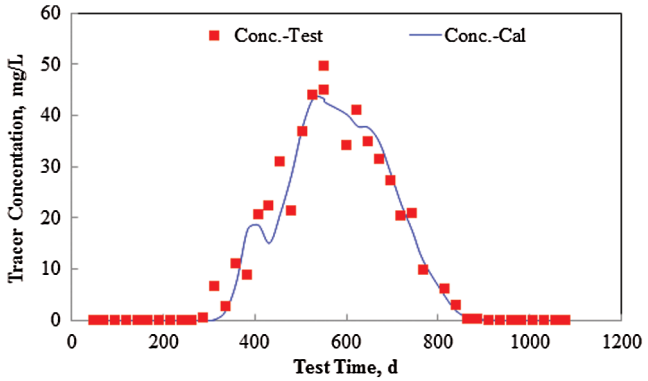

Figure 6: Field instance matched by the new model, Conc.-Test is the tracer test concentration, mg/L; Conc.-Cal is the tracer concentration calculated by the new model

To figure out effect of physical actions and fluid distribution on tracer concentration, Section 5 shows sensitivity analysis by proposed model.

5 Sensitivity analyses

5.1 Dispersion

As Fig. 7 shows, when mixing coefficient D increases from 0.01 to 0.06, the corresponding tracer concentration ratios break through earlier but increase more slowly. It results from that the dispersion tends to make tracer concentration distribution more uniform in water phase in flowing pores. Meanwhile, dispersion does not induce any mass loss, as shown in Fig. 7(b).

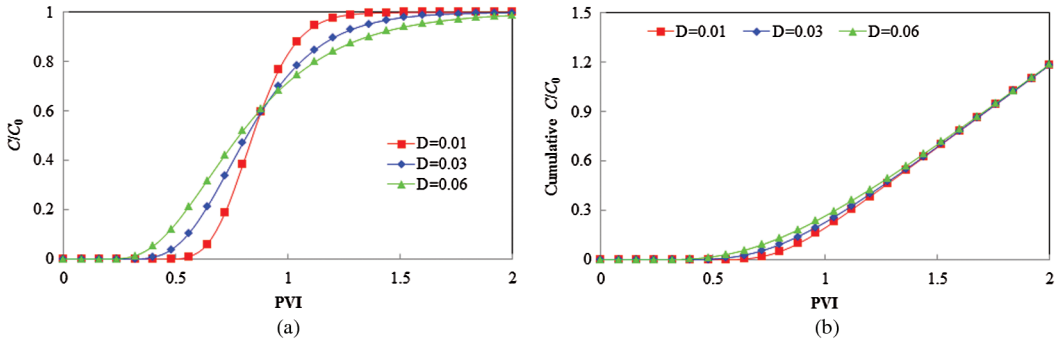

Figure 7: Tracer concentration *vs.* PVI at different mixing coefficient D (a) Tracer concentration ratio (b) Cumulative tracer concentration ratio

5.2 Adsorption

As Fig. 8(a) shows, when the adsorption coefficients increase from 0.01 to 0.08, the corresponding tracer concentration ratios break through later and increase more slowly. When the surface of flowing and storage pores adsorbs more tracers, it results in less cumulative tracer concentration, as shown in Fig. 8(b).

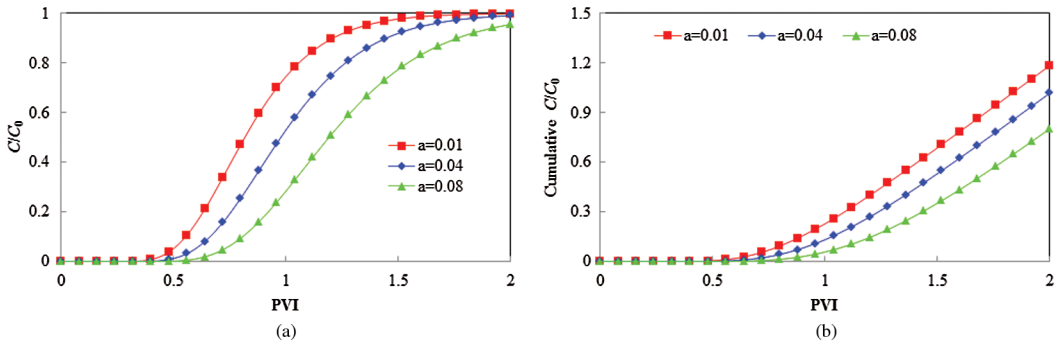

Figure 8: Tracer concentration *vs.* PVI at different adsorption coefficient a (a) Tracer concentration ratio (b) Cumulative tracer concentration ratio

5.3 Superficial velocity

As Fig. 9(a) shows, when tracer superficial velocity u' increases from 0.003 to 0.007 cm/s, the corresponding tracer concentration ratios break through later and increase more quickly, just contrast to the change laws of mixing coefficient D. On high superficial velocity, since the dispersion has less time to control tracer concentration distribution, the tracer breakthrough point becomes later versus PVI. Superficial velocity does not affect cumulative tracer concentration, as shown in Fig. 9(b).

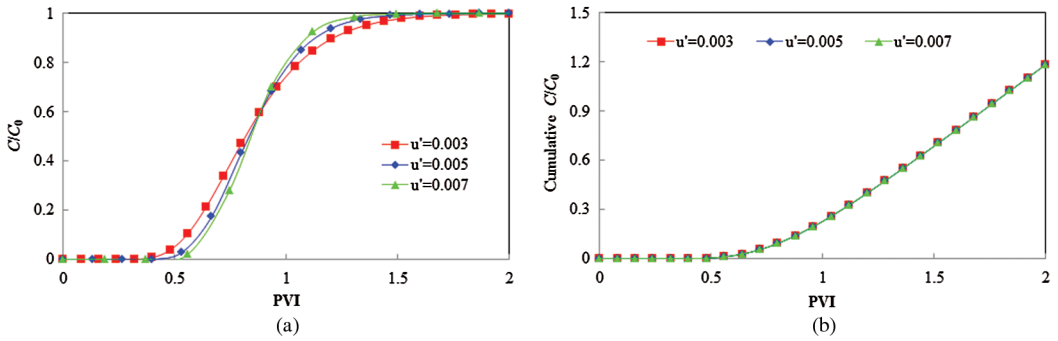

Figure 9: Tracer concentration *vs.* PVI at different tracer injected velocity u' (a) Tracer concentration ratio (b) Cumulative tracer concentration ratio

5.4 Bound water saturation

As Fig. 10(a) shows, when bound water saturation S_{wc} increases from 0 to 0.4, the corresponding tracer concentration ratios break through later and increase more quickly, just same with the change law of tracer superficial velocity u'. Same with the laws of tracer superficial velocity, S_{wc} has a positive correlation with the interstitial flow velocity and results that it is less time to control tracer concentration distribution for the dispersion as well. In continuous injection situation, bound water saturation has little effect on cumulative tracer concentration, as shown in Fig. 10(b).

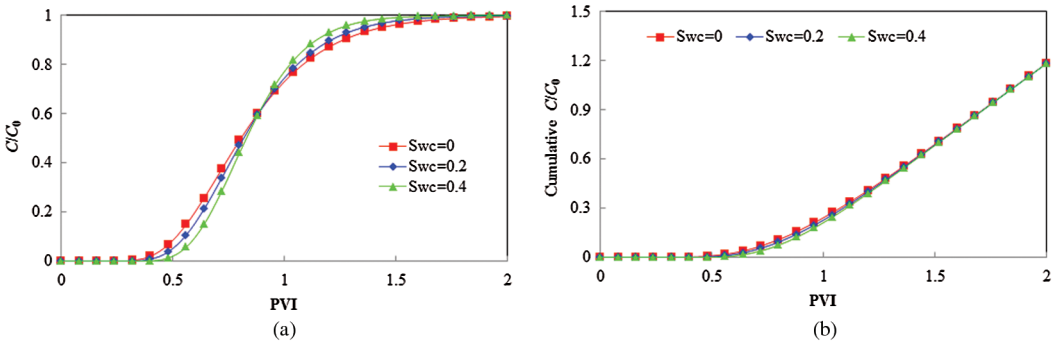

Figure 10: Tracer concentration *vs.* PVI at different tracer injected velocity S_{wc} (a) Tracer concentration ratio (b) Cumulative tracer concentration ratio

5.5 Flowing porosity

As Fig. 11(a) shows, when flowing porosity Φ_f increases from 0.1 to 0.3, the corresponding tracer concentration ratios break through earlier and increase more slowly. A larger Φ_f contributes more space for dispersion and results in same change law with higher dispersion coefficient. Fig. 11(b) illustrates that change of flowing porosity does not induce any mass loss.

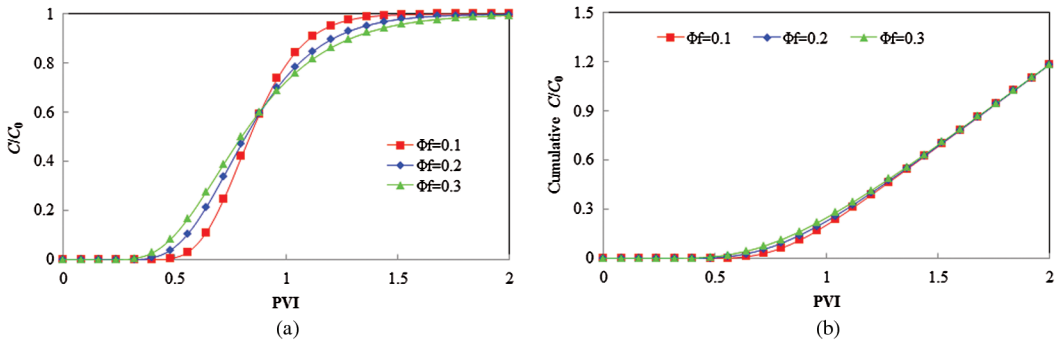

Figure 11: Tracer concentration *vs.* PVI at different tracer injected velocity Φ_f (a) Tracer concentration ratio (b) Cumulative tracer concentration ratio

6 Conclusions

Based on the microscopic experiments, the mechanisms of tracer in different types of pores are analyzed and characterized. Mathematical model for tracer transport is established and solved analytically by Laplace transform. The results of this study lead to the following conclusions:

(1) The microscopic experiments illustrate that injected tracer enters movable water first and then bound water in the flowing pores, indicating that it is necessary to consider the effect of bound water on tracer concentration distribution in mathematical modelling. Moreover, the injected tracer cannot occupy the storage pore completely until 5 PV injected, which is longer than that in the flowing pores. It indicates that flowing porosity has different effect on tracer concentration distribution if compared with total porosity. As microscopic experiments show, flowing and storage pores have different tracer behaviors, i.e., diffusion and adsorption in storage pores and advection, dispersion, diffusion and adsorption in flowing pores.

(2) The proposed mathematical model improves tracer transport description by considering bound water and flow porosity separately. The analytical solution of tracer concentration fits the experimental data better than that ignoring the effects of bound water and flowing porosity, with corresponding RSS=0.0005 and 0.0515, respectively.

(3) The dispersion coefficient and flowing porosity have a negative correlation with the tracer breakthrough time and the concentration growth rate, whereas the superficial velocity and bound water saturation have a positive correlation with them. The adsorption leads to a later breakthrough of tracer and a slower increase of concentration.

Acknowledgement: We gratefully acknowledge the work of Doc. Yi Wei.

Funding Statement: This research was funded by National Science and Technology Major Projects (2017ZX05009004, 2016ZX05058003), Beijing Natural Science Foundation

(2173061) and State Energy Center for Shale Oil Research and Development (G5800-16-ZS-KFNY005).

Conflicts of Interest: The authors declare no conflict of interest.

References

Al-Mosa, M. A.; Zaberi, H.; Huseby, O. (2013): Improved reservoir surveillance through injected tracers in a Saudi Arabian field: case study. *Society of Petroleum Engineers*. DOI 10.2118/166005-MS.

Al-Shalabi, E. W.; Luo, H.; Delshad, M.; Sepehrnoori, K. (2015): Single-well chemical tracer modeling of low salinity water injection in carbonates. *SPE Western Regional Meeting*.

Bellin, A.; Rinaldo, A. (1995): Analytical solutions for transport of linearly adsorbing solutes in heterogeneous formations. *Water Resources Research*, vol. 31, no. 6, pp. 1505-1511. DOI 10.1029/95WR00200.

Boving, T. B.; Grathwohl, P. (2001): Tracer diffusion coefficients in sedimentary rocks: correlation to porosity and hydraulic conductivity. *Journal of Contaminant Hydrology*, vol. 53, no. 1, pp. 85-100. DOI 10.1016/S0169-7722(01)00138-3.

Brigham, W. E.; Reed, P. W.; Dew, J. N. (1961): Experiments on mixing during miscible displacement in porous media. *Society of Petroleum Engineers Journal*, vol. 1, no. 01, pp. 1-8. DOI 10.2118/1430-G.

Cox, J. R.; Alsenani, M.; Miller, S. E.; Roush, J. A.; Shi, R. et al. (2017): Pyrolyzable nanoparticle tracers for environmental interrogation and monitoring. *ACS Applied Materials & Interfaces*, vol. 9, no. 15, pp. 13111-13120. DOI 10.1021/acsami.6b16050.

Dindoruk, D. M.; Dindoruk, B. (2008): Analytical solution of nonisothermal Buckley-Leverett flow including tracers. *SPE Reservoir Evaluation & Engineering*, vol. 11, no. 3, pp. 555-564. DOI 10.2118/102266-PA.

Gilfillan, S. M.; Sherk, G. W.; Poreda, R. J.; Haszeldine, R. S. (2017): Using noble gas fingerprints at the Kerr Farm to assess CO_2 leakage allegations linked to the Weyburn-Midale CO_2 monitoring and storage project. *International Journal of Greenhouse Gas Control*, vol. 63, pp. 215-225. DOI 10.1016/j.ijggc.2017.05.015.

Hanaor, D. A. H.; Ghadiri, M.; Chrzanowski, W.; Gan, Y. (2014): Scalable surface area characterization by electro kinetic analysis of complex anion adsorption. *Langmuir*, vol. 30, no. 50, pp. 15143-15152. DOI 10.1021/la503581e.

Huang, B.; Xu, R.; Fu, C.; Wang, Y.; Wang, L. (2018): Thief zone assessment in sandstone reservoirs based on multi-layer weighted principal component analysis. *Energies*, vol. 11, no. 5, pp. 1274-1287. DOI 10.3390/en11051274.

Huseby, O.; Hartvig, S. K.; Jevanord, K.; Dugstad, O. (2015): Assessing EOR potential from partitioning tracer data. *SPE Middle East Oil & Gas Show and Conference*.

Huseby, O.; Sagen, J.; Viig, S.; Dugstad, Ø.; Haugan, A. (2013): Simulation and interpretation of inter-well tracer tests. *EPJ Web of Conferences*, vol. 50, no. 2, pp. 03003. DOI 10.1051/epjconf/20135003003.

Jodar, J.; Medina, A.; Carrera, J. (2009): Gas tracer transport through a heterogeneous fracture zone under two phase flow conditions: model development and parameter sensitivity. *Advances in Water Resources*, vol. 32, no. 3, pp. 315-328. DOI 10.1016/j.advwatres.2008.10.008.

Kam, D.; Han, J.; Datta-Gupta, A. (2016): Streamline-based rapid history matching of bottom hole pressure and three-phase production data. *SPE Improved Oil Recovery Conference*.

Kocabas, I. (2011): Application of iterated Laplace transformation to tracer transients in heterogeneous porous media. *Journal of the Franklin Institute*, vol. 348, no. 7, pp. 1339-1362. DOI 10.1016/j.jfranklin.2010.04.002.

Krogstad, S.; Lie, K. A.; Nilsen, H. M.; Berg, C. F.; Kippe, V. (2017): Efficient flow diagnostics proxies for polymer flooding. *Computational Geosciences*, vol. 21, no. 5-6, pp. 1-16. DOI 10.1007/s10596-017-9681-9.

Lan, X. H. (2011): Research development on ocean isotope tracer technology. *Marine Geology Letters*, vol. 17, no. 11, pp. 6-9 (Chinese).

Li, C. (2014): The well-to-well tracer monitoring interpretation method research and application, Yangtze University (Chinese).

Li, J. J.; Jiang, H. Q.; Liu, T. J. (2010): Tracer transport in intra-formational water channeling reservoir. *Chinese Journal of Computational Physics*, vol. 27, no. 1, pp. 45-50. DOI 10.3724/SP.J.1016.20140.00045 (Chinese).

Li, J. J.; Liu, Y. Z.; He, P. C.; Jiang, H. Q. (2012): Analysis of tracer production characters after polymer flooding based on CTRW. *Journal of Daqing Petroleum Institute*, vol. 36, no. 1, pp. 47-52 (Chinese).

Li, J. Y.; Jiang, H. Q.; Li, J. J. (2010): Advection and dispersion laws of non-fractional tracer in porous media. *Oil-Gas field Surface Engineering*, vol. 29, no. 6, pp. 15-17 (Chinese).

Li, J. Y.; Jiang, H. Q.; Li, J. J.; Luo, X. B. (2011): Study on tracer dispersion influenced by polymer retention. *Petroleum Geology & Recovery Efficiency*, vol. 18, no. 4, pp. 78-81 (Chinese).

Liu, T. J.; Diwu, P. X.; Jiang, B. Y.; Liu, R.; Sun, L. (2013): Study on the assemble interpretation method of inter well tracer test. *China Mining Magazine*, vol. 22, no. suppl, pp. 210-213 (Chinese).

Liu, T. J.; Jiang, B. Y.; Liu, R.; Zhang, X. H.; Xie, X. Q. (2013): Experimental study on microcosmic visualization of tracer in porous medium. *Fault-Block Oil & Gas Field*, vol. 20, no. 4, pp. 530-534 (Chinese).

Liu, T. J.; Jiang, B. Y.; Liu, R.; Zhang, X. H.; Xie, X. Q. (2013): Reservoir characteristics of chromatographic effect of tracer flow in porous medium. *Journal of Chongqing University Natural Science Edition*, vol. 36, no. 9, pp. 58-63 (Chinese).

Liu, T. J.; Jiang, H. Q.; Li, N.; Lei, Z. X.; Li, X. S. (2008): Application of interwell tracer testing in describing remaining oil distribution. *Petroleum Geology & Oilfield Development in Daqing*, vol. 27, no. 1, pp. 74-77 (Chinese).

Liu, T. J.; Jiang, H. Q.; Li, X. S.; Lei, Z. X.; Zhao, J. L. et al. (2007): Semi-analytical mathematical model for well-to-well tracer test system. *Acta Petrolei Sinica*, vol. 28, no. 5, pp. 118-123. DOI 10.1111/j.1745-7254.2007.00484.x (Chinese).

Liu, T. J.; Zhang, X. H.; Jiang, H. Q.; Dai, X. B.; Zhang, P. X. (2007): New advance on the tracer test technology among wells. *Journal of Isotopes*, vol. 20, no. 3, pp. 189-192 (Chinese).

Mennella, A.; Bryant, S. L.; Lockhart, T. P. (1999): Analysis of high-dispersion tracer tests in cores containing polymer gels. *Journal of Petroleum Science and Engineering*, vol. 23, no. 3, pp. 201-212. DOI 10.1016/S0920-4105(99)00017-0.

Nihoul; Jacques, C. J. (1983): Analytical solutions of the one-dimensional connective-dispersive solute transport equation. *Ecological Modelling*, vol. 19, no. 3, pp. 222-223. DOI 10.1016/0304-3800(83)90057-1.

Rein, E.; Schulz, L. K. (2007): Applications of natural gas tracers in the detection of reservoir compartmentalisation and production monitoring. *Journal of Petroleum Science and Engineering*, vol. 58, no. 3-4, pp. 428-442. DOI 10.1016/j.petrol.2005.11.020.

Scher, H.; Lax, M. (1973a): Stochastic transport in a disordered solid. I. Theory. *Physical Review B*, vol. 7, no. 10, pp. 4491-4502. DOI 10.1103/PhysRevB.7.4491.

Scher, H.; Lax, M. (1973b): Stochastic transport in a disordered solid. II. Impurity conduction. *Physical Review B*, vol. 7, no. 10, pp. 4502-4519.

Semra, S.; Sardin, M.; Simonnot, M. O. (2008): Effect of chemical heterogeneity on adsorbed solute dispersion at column scale. *AIChE Journal*, vol. 54, no. 4, pp. 950-956. DOI 10.1002/aic.11437.

Singh, A. K.; Pilz, P.; Zimmer, M.; Kalbacher, T.; Görke, U. J. et al. (2012): Numerical simulation of tracer transport in the Altmark gas field. *Environmental Earth Sciences*, vol. 67, no. 2, pp. 537-548. DOI 10.1007/s12665-012-1688-x.

Stalgorova, E.; Babadagli, T. (2012): Field-scale modeling of tracer injection in naturally fractured reservoirs using the random-walk particle-tracking simulation. *SPE Journal*, vol. 17, no. 2, pp. 580-592. DOI 10.2118/144547-PA.

Widiatmojo, A.; Sasaki, K.; Yousefi-Sahzabi, A.; Nguele, R.; Sugai, Y. et al. (2015): A grid-free particle tracking simulation for tracer dispersion in porous reservoir model. *Journal of Unconventional Oil and Gas Resources*, vol. 11, pp. 75-81. DOI 10.1016/j.juogr.2015.05.005.

Yang, H. B.; Shao, S.; Zhu, T.; Chen, C.; Liu, S. et al. (2019): Shear resistance performance of low elastic polymer microspheres used for conformance control

treatment. *Journal of Industrial and Engineering Chemistry*, vol. 79, pp. 295-306. DOI 10.1016/j.jiec.2019.07.005.

Yang, S. R.; Liu, T. J. (2007): Brief introduction on interwell tracer test with micro-material. *Well Logging Technology*, vol. 31, no. 5, pp. 408-412 (Chinese).

Yang, X. (2012). *Interpretation Method of Single Well Tracer Test for Formation Heterogeneity (Master Thesis)*, Southwest Petroleum University, China (Chinese).

Zha, F. (2010): *Interpretation Method Research for Well-Group Tracer Production Curves (Master Thesis)*, China University of Petroleum (East China), China (Chinese).

Zhang, X. H.; Liu, T. J.; Zhang, P. X.; Gao, Y.; Li, J. F. et al. (2005): The interwell tracer test interpretation in the Tarim Donghe oil field. *Journal of Isotopes*, vol. 18, no. 2, pp. 9-14 (Chinese).